

# Excitation laser fluence effects on the $\text{Ba} \cdots \text{FCH}_3 + h\nu \rightarrow \text{BaF} + \text{CH}_3$ intracluster reaction

A. González Ureña<sup>\*</sup>, K. Gasmi, J. Jiménez, R.F. Lobo<sup>1</sup>

*Unidad de Láseres y Haces Moleculares, Instituto Pluridisciplinar, Universidad Complutense de Madrid, P<sup>a</sup> Juan XXIII-1<sup>o</sup>,  
28040 Madrid, Spain*

Received 18 October 2001; in final form 4 December 2001

---

## Abstract

In this work, results on the  $\text{Ba} \cdots \text{FCH}_3 + h\nu \rightarrow \text{BaF} (\text{Ba}^*) + \text{CH}_3 (\text{CH}_3\text{F})$  reaction obtained under high laser field conditions are reported. We have found that the two-photodissociation channel yields, i.e. the reactive BaF and non-reactive Ba<sup>\*</sup> products, exhibited opposite behaviour depending upon the laser fluence. Whereas the BaF yield rises as the laser fluence is increased, the Ba<sup>\*</sup> yield decreases over the same laser fluence range. In other words, the product (Ba<sup>\*</sup>)/(BaF) branching ratio changes significantly from low to high laser fluence in such a way that the (photoinitiated)  $\text{Ba} \cdots \text{FCH}_3 \rightarrow \text{BaF} + \text{CH}_3$  reaction may be controlled by changing the intensity of the excitation laser field. © 2002 Elsevier Science B.V. All rights reserved.

---

## 1. Introduction

Laser control of chemical reactions is currently attracting a considerable attention from both theoretical and experimental point of view [1–3]. Among several schemes to implement the control of a chemical reaction one of the most promising is based on quantum interference control mostly applied to unimolecular reactions. For this type of processes, in which a single re-

actant molecule is transformed to several product molecules, two types of control have been applied. Namely, the ‘two-beam interference control’ [4–6] and the ‘two-pulse time delay control’ [3,7,8]. While in the former case control is achieved by quantum interference between different reaction pathways relating the same initial and final states, the latter method uses a variable time delay between two extremely short light pulses.

In the present work, we report on the control of the (photoinitiated)  $\text{Ba} \cdots \text{FCH}_3 + h\nu \rightarrow \text{BaF} + \text{CH}_3$  intracluster reaction achieved by changing the fluence of the excitation laser. Pioneering work on photofragmentation of  $\text{Fe}(\text{H}_2\text{O})_n^+$  clusters ( $n = 1\text{--}9$ ) as a function of the laser fluence at different wavelengths was carried out by Mest-

---

<sup>\*</sup> Corresponding author. Fax: +34-1-39-43265.

E-mail addresses: [laseres@eucmax.sim.ucm.es](mailto:laseres@eucmax.sim.ucm.es), [laseres@pluri.ucm.es](mailto:laseres@pluri.ucm.es) (A. González Ureña).

<sup>1</sup> Present address: Departamento de Física, Faculdade de Ciências e Tecnologia, Universidade Nova de Lisboa, Quinta da Torre 28025, Monte de Caparica, Lisboa, Portugal.

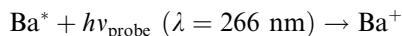
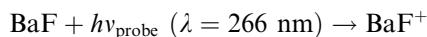
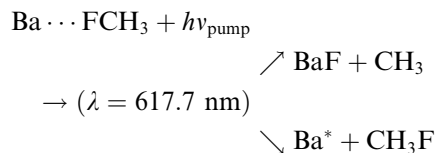
dagh and co-workers [9]. Linear dependence of cross-sections ( $0.05 \text{ \AA}^2$ ) was always found even at fluences up to  $100 \text{ mJ/cm}^2$ . Here the two photo-fragmentation channels i.e., reactive BaF and non-reactive  $\text{Ba}^*$ , yields exhibited opposite behaviour depending upon the laser fluence. Indeed, whereas the BaF yield increases with increasing laser fluence, the  $\text{Ba}^*$  yield decreases over the same laser fluence range. In other words, the product  $[\text{Ba}^*]/[\text{BaF}]$  branching ratio changes significantly from low to high laser fluence conditions. It is emphasised that we used nanosecond laser pulses being the excitation laser fluence the only adjustable variable. The simplicity of this scheme could also be of interest for practical applications.

## 2. Experimental

A detailed description of the molecular beam apparatus is given elsewhere [10,11] and only a brief description will be presented here. The weakly bound complex  $\text{Ba} \cdots \text{FCH}_3$  is produced in a laser vapourisation source followed by supersonic expansion, using a gas mixture of He with a 10% of  $\text{CH}_3\text{F}$ . The molecular beam is then probed in a different chamber using a laser ionisation coupled with a linear time-of-flight mass spectrometer.

Two lasers are used for the probing of the molecular beam. A tunable laser induces the reaction in the  $\text{Ba} \cdots \text{FCH}_3$  weakly bound complex while a second laser ionises the complex and the  $\text{Ba} \cdots \text{FCH}_3$  photofragmentation products. An infinity-XPO laser with a bandwidth of typical  $5 \text{ cm}^{-1}$  and a pulse duration of 3.5 ns is used for excitation of the complex, while the fourth harmonic of a Continuum NY80 Nd:YAG laser (266 nm, pulse duration 7 ns) is used for ionisation. The excitation laser arrives about 7–10 ns earlier to the beam-laser interaction region than the ionisation laser. This is achieved using an electronic delay generator provided by the infinity-XPO laser.

The pump and probe scheme used in the present experiment is the following:



The  $\text{BaF}^+$  signal is produced by direct one photon ionisation of BaF product absorption of the 266 nm photon, as demonstrated in previous work (see for example Fig. 2 of [12]). With respect to the  $\text{Ba}^*$  product, direct one photon ionisation of

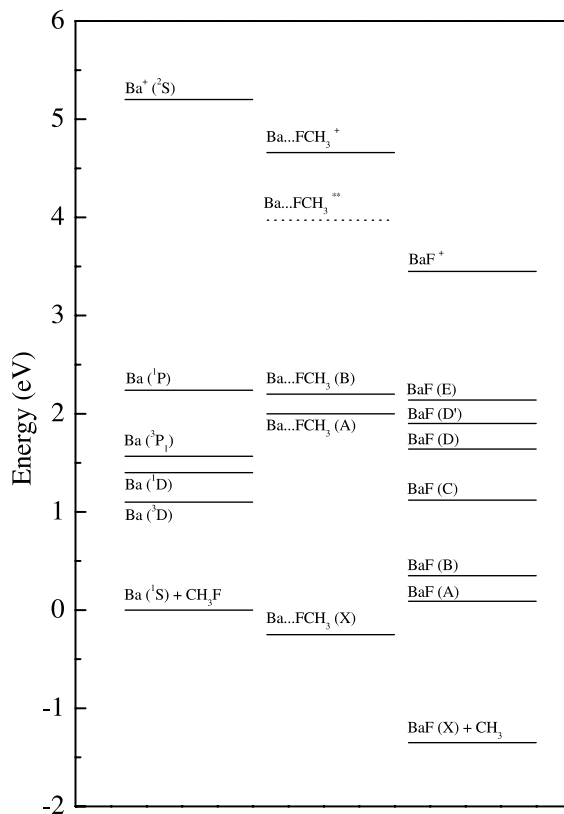


Fig. 1. Energy level diagram of the  $\text{Ba} + \text{CH}_3\text{F}$  system. The left column shows the Ba electronic energy levels and the right one the BaF energy levels. The centre column displays an approximate location of the  $\text{Ba} \cdots \text{FCH}_3$  electronic states including the hypothetical  $(\text{Ba} \cdots \text{FCH}_3)^{**}$  Rydberg state. See text for comments.

Ba ground state is not possible at 266 nm, so only metastable  $\text{Ba}^*$  product can be ionised. See Fig. 1 for an energy diagram of the system here investigated. Under the present experimental conditions the 266 nm probing laser intensity was always kept at a very low intensity to guarantee that two-photon absorption process was, if any, a very minor effect. It should be recalled that the pumping laser wavelength excites the  $A \leftarrow X$  electronic transition of the  $\text{Ba} \cdots \text{FCH}_3$  complex only, i.e., it does not affect the free Ba atoms present in the beam expansion at all (see [11] for details).

The experiment consisted of measuring simultaneously the  $\text{BaF}^+$  and  $\text{Ba}^+$  signals at two different conditions: (a) using UV photons ( $\lambda = 266$  nm) and (b) using first a pump XPO laser ( $\lambda = 617.7$  nm) and then, 10 ns later, the UV ( $\lambda = 266$  nm) laser. The  $\text{BaF}$  and  $\text{Ba}^*$  action signals were estimated from their, (b) minus (a) signals, respectively. This procedure was then repeated at different XPO laser fluences. The latter was modified by using a high energy variable attenuator (Newport mod. 935-5-OPT). This procedure ensured that the focus and optical features of the laser beam remained unchanged.

### 3. Results and discussion

Fig. 2 (solid line) shows a time-of-flight mass spectrum of the  $\text{Ba} + \text{FCH}_3$  system when the fundamental output of the Nd:YAG is used for vapourisation and the species in the beam are ionised with the 266-nm radiation. A significant depletion of the monomer signal is observed when the excitation OPO laser is tuned to 617.7 nm and allowed to enter into the detection chamber (dashed line). It should be indicated that no depletion is observed for other species contained in the beam, indicating that these should probably absorb at different wavelengths. Furthermore the enhancement of both Ba and  $\text{BaF}$  signals is clearly noticed due to complex photofragmentation (see [12,13] for further details).

As for the  $\text{Ba}^*$  signal, it should be emphasised that no  $\text{Ba}^*$  ion signal was observed with the pump laser only, even though higher fluences were employed. Thus, taking into consideration the energetic diagram, one can conclude that the non-reactive photofragmentation channel here investigated, with the  $\lambda = 266$  nm probing, corresponds to metastable  $\text{Ba}(^1\text{D}_1, ^3\text{P})$  states.

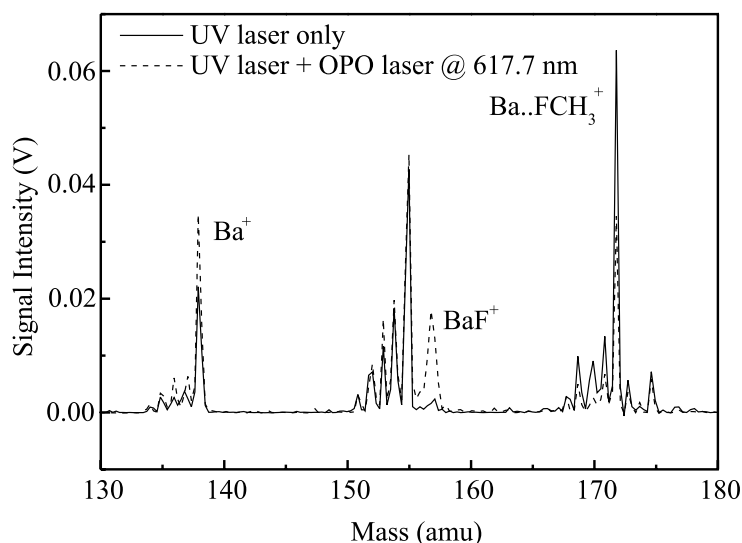


Fig. 2. Solid line: time-of-flight mass spectra of the  $\text{Ba} + \text{CH}_3\text{F}$  system. Strong depletion of the  $\text{Ba} \cdots \text{FCH}_3$  complex is observed when the OPO laser is tuned to 617.7 nm. The enhancement of both Ba and  $\text{BaF}$  signals is also clearly noticed as a result of the complex photofragmentation.

The individual photofragmentation channel yields are displayed on Figs. 3 and 4 as a function of the laser fluence. Both  $\Delta\text{Ba}^*$  and  $\Delta\text{BaF}$  signals were obtained using the same procedure. The  $\Delta\text{Ba}^*$  was calculated by subtracting the  $\text{Ba}^*$  (UV) signal from the  $\text{Ba}^*$  (UV + VIS). Here UV and VIS stand for the signal measured when the UV ( $\lambda = 266$  nm) and XPO ( $\lambda = 617.7$  nm) laser were employed, respectively. The most interesting feature is the laser fluence dependence of both reactive,  $\Delta\text{BaF}$ , and non-reactive,  $\Delta\text{Ba}^*$ , yields. While  $\Delta\text{Ba}^*$  increases reaching a maximum around  $1.9 \text{ mJ/cm}^2$  with a subsequent decline beyond this fluence value, the  $\Delta\text{BaF}$  always increases over the studied laser fluence range. Clearly, the  $[\text{Ba}^*]/[\text{BaF}]$  branching ratio as depicted in Fig. 5 is not con-

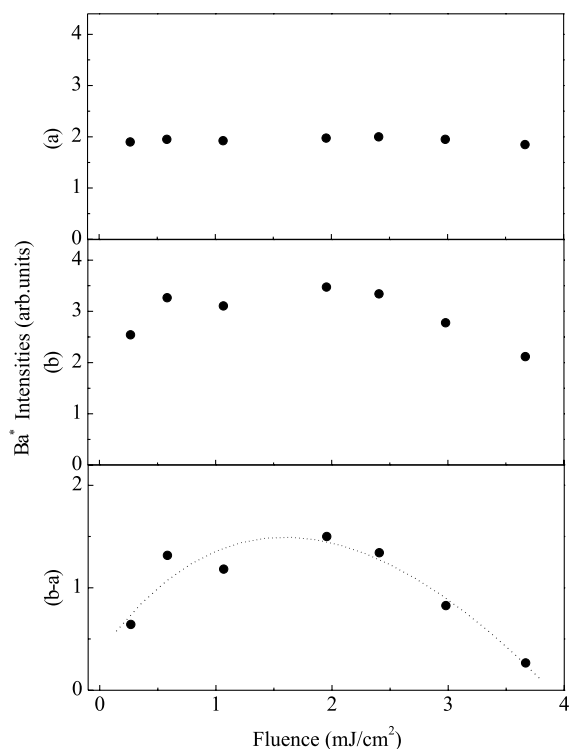


Fig. 3.  $\text{Ba}^*$  photofragmentation yield ratios as a function of the laser fluence. (a)  $\text{Ba}^*$  signal with the UV laser, (b)  $\text{Ba}^*$  signal when VIS pump laser operated 10 ns before the probe UV laser arrives to the ionisation region.  $\Delta\text{Ba}^*$  signal obtained by subtracting (a) from (b) signal. In all cases the same relative units are used.

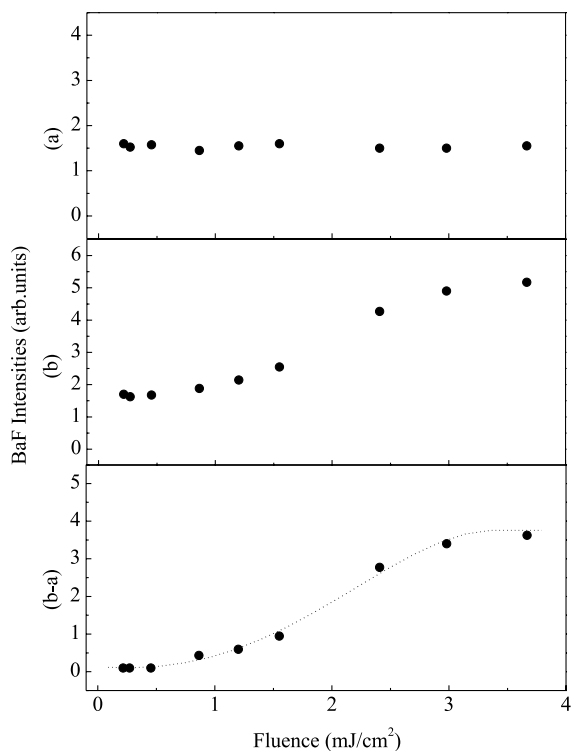


Fig. 4. Same presentation as in Fig. 3, but now for the BaF channel. Notice the opposite behaviour of the present BaF channel when compared with previous  $\text{Ba}^*$  data, in particular for laser fluences beyond  $\sim 2 \text{ mJ/cm}^2$ .

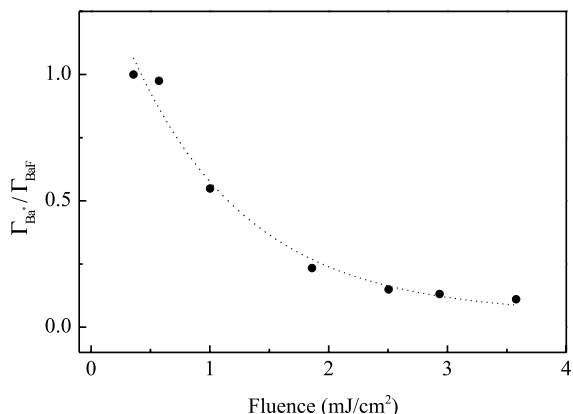
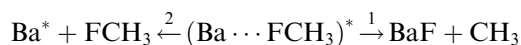


Fig. 5. Laser fluence dependence of the  $[\text{Ba}^*]/[\text{BaF}]$  branching ratio. Points: present experimental results; dotted line is just a guide to the eye.

stant but depends of the laser field employed to induce the reaction.

For an understanding of the present results it should be remarked that as the complex is irradiated with more and more photons a coherent superposition of both ground and excited states is created. In addition, the  $\text{Ba} \cdots \text{FCH}_3$  decomposes via two channels, e.g.



and consequently the lifetime of the excited  $(\text{Ba} \cdots \text{FCH}_3)^*$  may be influenced not only by the two channel photofragmentation dynamics but also by the intense laser field conditions. In this view, the actual  $(\text{Ba} \cdots \text{FCH}_3)^*$  concentration is not longer constant but follows a periodical time dependent functionality controlled by the Rabi frequency and so by the laser fluence  $F$ . Indeed  $[\text{Ba} \cdots \text{FCH}_3^*]$  will vary as  $\sim \sin^2(\Omega/2)t$ , in which the Rabi frequency,  $\Omega$ , is proportional to  $\sim F^{1/2}$  (hereafter we will write  $\Omega = aF^{1/2}$ ,  $a$  being a laser fluence independent parameter). The coherent superposition of complex excited and ground states leads to a shortening of its lifetime which may favour the faster photodissociation channels as  $F$ , and so  $\Omega$ , increases. As a result, photofragmentation products could be selectively formed as long as the reaction time is comparable with the Rabi period  $1/\Omega$ . It is out of the scope of the present Letter to describe the calculation of the transition moment and the Rabi frequency for the studied transition as a function of the laser fluence. However, as it will be published elsewhere [14], the Rabi period lies about the picosecond time domain over the low laser fluence range used in the present experiment, reaching the sub-picosecond regime at high fluences [14]. To the best of our knowledge there is no experimental information about the reaction time associated to the non-reactive channel yielding  $\text{Ba}^*$  products. However, the reaction time for the  $\text{BaF}$  channel has been measured to be about 270 fs by the femtosecond pump and probe technique [15,16]. Thus one can assume that the reaction time for the non-reactive channel could well be of the order of picoseconds as it is the (usual) case in photodissociation dynamics of van der Waals molecules. Bearing all this in mind, it seems that the employed laser conditions are

probably suitable to achieve the control of the intracuster reaction by changing the laser fluence.

One of the crucial questions concerning the interpretation of present results is whether or not a multiphoton process is controlling the fluence dependence of the different reaction channels, because if such a process was present it could open new routes to turn on the reaction and produce the  $\text{BaF}$ . In this view, the enhancement of the  $\text{BaF}$  yield, as the laser fluence increases, would reflect the predominance of this new route rather than the (favoured) faster photofragmentation channel due to the shortening of the (excited complex) lifetime as the Rabi frequency increases. This alternative is further discussed below.

Let us consider for example the absorption of two-photon by the  $\text{Ba} \cdots \text{FCH}_3$  complex. A two-photon mechanism would put  $36.283 \text{ cm}^{-1}$  into the system. As can be seen in the energetic diagram of Fig. 1 this would form a  $\text{Ba}^+ \cdots \text{CH}_3\text{F}$  ion surrounded by the Rydberg electron in a different orbital. In principle this state might evolve to form  $\text{BaF}^+ \cdots \text{CH}_3$  underneath the Rydberg state and subsequently  $\text{BaF}^* + \text{CH}_3$ . Thus, this  $\text{BaF}^*$  could then be easily excited by the probe ( $\lambda = 266 \text{ nm}$ ) photon.

The  $\text{Ba} \cdots \text{FCH}_3$  absorption at 618 nm was studied in [16] (see, for example, its Section 3.1), monitoring the strong peak of the  $\text{Ba} \cdots \text{FCH}_3^+$  signal caused by the simultaneous absorption of the one pump photon ( $\lambda = 618 \text{ nm}$ ) and one probe photon ( $\lambda = 400 \text{ nm}$ ). Typical values of the (120 fs) pump and probe laser fluences were 0.5 and  $1 \text{ mJ/cm}^2$ , respectively. For the pump laser the used fluence of  $0.5 \text{ mJ/cm}^2$  and 120 fs pulse duration gave a laser intensity of ca.  $4 \times 10^9 \text{ W/cm}^2$ . As reported in [16] a linear dependence was always found for each photon over a range of 4 in laser fluence.

Obviously, the comparison between the possible two-photon regime induced in the present nanosecond experiment and previous [16] femtosecond experiment must integrate the pulse duration. Taking the latter into account one can show that the two-photon absorption process would therefore be much less probable in the present experiment than in the previously reported femtosecond study [16].

On the other hand, the possibility that such  $(\text{Ba} \cdots \text{FCH}_3)^{**}$  Rydberg state leads into  $\text{BaF} + \text{CH}_3$  through  $\text{Ba}^+ \cdots \text{FCH}_3 \rightarrow \text{BaF}^+ + \text{CH}_3$  reaction underneath of the Rydberg electron seems very unlikely. The  $(\text{Ba} \cdots \text{FCH}_3)^+$  seems to be a very stable ion. When the  $\text{Ba} \cdots \text{FCH}_3$  ionisation potential (see Fig. 4 in [11]) was measured, the  $\text{Ba} \cdots \text{FCH}_3^+$  signal increased smoothly with the laser ionisation energy even though the  $\text{BaF}^+ + \text{CH}_3$  channel was energetically opened (see energetic diagram), which can only be interpreted as that the  $\text{Ba} \cdots \text{FCH}_3^+$  fragmentation into  $\text{BaF}^+ + \text{CH}_3$  should be a very minor channel, at least at present excitation energies.

In summary, taking all the above considerations into account we conclude that multiphoton processes can be ruled out under the present experimental conditions.

#### 4. Concluding remarks

The most interesting finding of the present work is that the  $(\text{Ba} \cdots \text{FCH})^*$  two-photodissociation channel yields, i.e. the reactive  $\text{BaF}$  and non-reactive  $\text{Ba}^*$  products, exhibited opposite behaviour depending upon the laser fluence. The  $\text{BaF}$  yield rises as the laser fluence is increased. However, the  $\text{Ba}^*$  yield reached a maximum at low fluences with a subsequent decline over the high laser fluence range. This opposite behaviour was attributed to a different reaction times associated to each individual photofragmentation channel of the  $\text{Ba} \cdots \text{FCH}_3$ . In this picture, the faster channel, the  $\text{BaF}$  product, would be favoured with respect to the slower one, the  $\text{Ba}^*$  product, as the excited complex lifetime becomes shorter as the Rabi frequency increases. This would justify the observation that the product  $(\text{Ba}^*)/(\text{BaF})$  branching ratio changes significantly from low to high laser fluence in such a way that the (photoinitiated)  $\text{Ba} \cdots \text{FCH}_3 + h\nu \rightarrow \text{BaF} + \text{CH}_3$  reaction could be controlled.

A key feature of the present investigation is the use of nanosecond laser pulses with the excitation

laser fluence as the only adjustable parameter to achieve the control of the photoinitiated reaction. Furthermore the application to a bimolecular reaction by clustering the reactants in a van der Waals should also be remarked. The simplicity of this scheme could be of interest when one considers its potentiality for practical applications.

#### Acknowledgements

The authors acknowledge helpful discussions with J.M. Mestdagh on the results presented in this work. This work received financial support from DGES of Spain Grant PB97-0272 and the Ramón Areces Foundation.

#### References

- [1] R.N. Zare, *Science* 279 (1998) 1875.
- [2] S.A. Rice, *Nature* 409 (2000) 422.
- [3] A. Assion, T. Baumert, M. Bergt, T. Brixner, B. Kiefer, V. Seyfried, M. Strehle, G. Gerber, *Science* 282 (1998) 919.
- [4] M. Shapiro, P.J. Brumer, *J. Chem. Phys.* 84 (1986) 4103.
- [5] M. Shapiro, P.J. Brumer, *J. Chem. Phys.* 97 (1992) 6259.
- [6] L.-C. Zhu, V. Kleiman, X.-N. Li, S.P. Lu, K. Trentelman, R.J. Gordon, *Science* 270 (1995) 77.
- [7] D. Tannor, S.A. Rice, *J. Chem. Phys.* 83 (1985) 5013.
- [8] T. Baumert, M. Grosser, R. Thalweiser, G. Gerber, *Phys. Rev. Lett.* 67 (1991) 3753.
- [9] L. Dukan, L. del Fabbro, P. Pradel, O. Sublemontier, J.M. Mestdagh, J.P. Visticot, *Eur. Phys. J. D* 3 (1998) 257.
- [10] S. Skowronek, R. Pereira, A. González Ureña, *J. Chem. Phys.* 107 (1997) 1668.
- [11] S. Skowronek, R. Pereira, A. González Ureña, *J. Phys. Chem.* 101 (1997) 7468 (Special issue on Stereodynamics).
- [12] S. Skowronek, A. González Ureña, in: R. Campargue (Ed.), *Atomic and Molecular Beams: The State of the Art*, Springer, Berlin, 2000, p. 353.
- [13] S. Skowronek, A. González Ureña, *Prog. React. Kinet. Mech.* 24 (1999) 101.
- [14] A. González Ureña et al., in preparation.
- [15] V. Stert, P. Farmanara, W. Radloff, F. Noack, S. Skowronek, J. Jimenez, A. González Ureña, *Phys. Rev. A* 59 (3) (1999) 1727.
- [16] P. Farmanara, V. Stert, W. Radloff, S. Skowronek, A. González Ureña, *Chem. Phys. Lett.* 304 (1999) 127.